

Computer Aided X-Ray Diffraction Intensity Analysis for Spinel: Hands-On Computing Experience

Ashish R. Tanna and Hiren H. Joshi

Abstract—The mineral having chemical compositional formula MgAl_2O_4 is called “spinel”. The ferrites crystallize in spinel structure are known as spinel-ferrites or ferro-spinels. The spinel structure has a *fcc* cage of oxygen ions and the metallic cations are distributed among tetrahedral (A) and octahedral (B) interstitial voids (sites). The X-ray diffraction (XRD) intensity of each Bragg plane is sensitive to the distribution of cations in the interstitial voids of the spinel lattice. This leads to the method of determination of distribution of cations in the spinel oxides through XRD intensity analysis. The computer program for XRD intensity analysis has been developed in C language and also tested for the real experimental situation by synthesizing the spinel ferrite materials $\text{Mg}_{0.6}\text{Zn}_{0.4}\text{Al}_x\text{Fe}_{2-x}\text{O}_4$ and characterized them by X-ray diffractometry. The compositions of $\text{Mg}_{0.6}\text{Zn}_{0.4}\text{Al}_x\text{Fe}_{2-x}\text{O}_4$ ($x = 0.0$ to 0.6) ferrites have been prepared by ceramic method and powder X-ray diffraction patterns were recorded. Thus, the authenticity of the program is checked by comparing the theoretically calculated data using computer simulation with the experimental ones. Further, the deduced cation distributions were used to fit the magnetization data using Localized canting of spins approach to explain the “recovery” of collinear spin structure due to Al^{3+} - substitution in Mg-Zn ferrites which is the case if A-site magnetic dilution and non-collinear spin structure. Since the distribution of cations in the spinel ferrites plays a very important role with regard to their electrical and magnetic properties, it is essential to determine the cation distribution in spinel lattice.

Keywords—Spinel ferrites, Localized canting of spins, X-ray diffraction, Programming in Borland C.

I. INTRODUCTION

THE general chemical composition of spinel ferrites is $\text{MO} \cdot \text{Fe}_2\text{O}_3$ and can be derived from magnetite $\text{Fe}^{2+}\text{O} \cdot \text{Fe}_2^{3+}\text{O}_3$ by the replacement of the Fe^{2+} ion by other divalent ions like Ni, Co, Cu, Zn, Cd, etc. It is also possible to replace Fe^{3+} by ions like Al^{3+} , Ga^{3+} , Cr^{3+} , etc. A monovalent ion Li^+ can be introduced in the spinel structure provided a trivalent ion is simultaneously introduced for charge balance. In the spinel structure there are two different types of interstitial sites: tetrahedral (A) and octahedral (B), which are occupied by different metal ions. In general, the magnetic interactions between these metal ions, limited only to the nearest neighbors, are antiferromagnetic in nature and their magnitudes are given by exchange integrals: J_{AA} , J_{BB} , J_{AB} .

Ashish R. Tanna is with the RK University, Rajkot 360020 INDIA (phone: +91-942-755-0255; e-mail: ashishrtanna@gmail.com).

Hiren H. Joshi is Head at Department of Physics, Saurashtra University, Rajkot 360005 INDIA (e-mail: joshihh@gmail.com).

When the two sub lattices (A and B) are occupied by the magnetic ions of the same type, the relative strengths are given by $|J_{AB}| > |J_{BB}| > |J_{AA}|$.

Thus, the magnetic moments on A and B-sites are aligned antiparallel to each other and this impels the two AA and BB moments to be parallel despite the antiferromagnetic exchange interactions between them, so these moments are in frustrated state. This is the scenario of the simple ferrimagnetic type of long range ordering. A number of ferrimagnetic spinels show the observed value of saturation magnetization much lower than that predicted by the Neel's collinear spin theory [1]. Yafet and Kittel [2] were the first to argue that non-magnetic substitutions on one sublattice could lead to a non-collinear or uniformly canted spin arrangement on the other sublattice. Rosenzweig [3],[4] presented a localized variant of the Yafet-Kittel calculation in which nearest neighbour exchange parameters were kept constant and local nearest neighbour statistics were used to obtain local effective molecular field and local canting angles. Patton and Liu [5] provided a mathematical formulation of Random Localized Canting and also the algorithm for the evaluation of the average canting angles on site to site basis.

One can in principle alter the relative strengths of all the exchange integrals by changing the type the magnetic ions on A and B sites and also disturbs the long range ferrimagnetic ordering. This implies that the knowledge of cation distribution is essential to understand the magnetic properties of spinel ferrites.

It is known that in X-Ray Diffraction (XRD) pattern the intensity of diffracted beam is determined by the type and distribution of the cations in the interstitial voids of the lattice [6],[7]. The XRD facility is easily accessible compared to the other experimental techniques like neutron diffraction, ^{57}Fe Mossbauer spectroscopy (which gives Fe^{3+} distribution) and X-ray Photoelectron Spectroscopy (XPS).

The cation distribution computer program using x-ray diffraction intensity based on algorithm (Fig. 1) is developed in C-language. The executable file (Intensity.exe) is generated to run the program. To operate this program, one has to insert input file after running the program. (Input file format is given). Input file included information like: (i) spinel ferrite system (ii) cations symbols (iii) tentative cations distribution values among interstitial sites (iv) X-ray's wavelength etc.

After the development of X-ray diffraction (XRD) intensity analysis computer program, it was thought worthwhile to synthesize a spinel system for real application of the computer

program. Al^{3+} renders good contrast in terms X-ray atomic scattering factor in the presence of Zn^{2+} , Fe^{2+} and Mg^{2+} [6]. This leads to the selection of spinel system $\text{Zn}_{0.4}\text{Mg}_{0.6}\text{Al}_x\text{Fe}_{2-x}\text{O}_4$ ($x = 0.0$ to 0.6 , step = 0.1) for testing the program and the compositional behavior of its structural, magnetic and electrical properties.

II. THEORY AND ALGORITHM FOR X-RAY DIFFRACTION INTENSITY CALCULATION COMPUTER PROGRAM

A. Spinel Structure

Spinel ferrites have crystal structure of compounds with the general formula AB_2X_4 [A and B are cations; X is an anion (O, S, Se, Te)], which crystallize with the same atomic structure as the mineral spinel, MgAl_2O_4 . Three degree of freedom associated with the detailed atomic arrangements of spinels are (i) the lattice parameter, a ; (ii) the anion parameter, u ; and (iii) the cation inversion parameter, i . Oxide spinels are used as example to explore the interrelationships between these parameters.

Many spinels exhibit remarkable electrical, magnetic, structural and other physical characteristics. Bragg [8] determined the crystal structure of spinel independently. The majority of spinel compounds belong to space group $\text{Fd}\bar{3}\text{m}$. the primitive tetrahedral unit cell of spinel is illustrated in Fig. 1. This cell consists of two molecular AB_2X_4 units and is presented by two octants in Fig. 1, with atomic positions indicated in the diagram. Four primitive unit cells, arranged as shown in Fig. 1, combine to form the conventional, cubic unit cell of spinel. Consequently, there are $Z=8$ formula units per cubic unit cell, each of which consist of 32 anions and 24 cations, for a total of 56 atoms. The Bravais lattice of the conventional unit cell is face-centered cubic (fcc); the basis consists of two formula units.

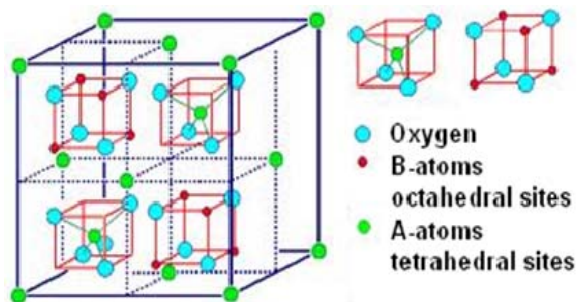


Fig. 1 Spinel structure with tetrahedral (A) & octahedral (B) sites

The anion sublattice is arranged in a pseudo-cubic close packed (cpp) spatial arrangement, although some spinels possess almost ideal ccp anion sub lattices. The repeat unit of the conventional unit cell is twice that of the anion lattice. As a consequence, the spinel lattice parameters (a) are large. In natural MgAl_2O_4 , $a = 0.80898(9)$ nm.

There are 96 interstices between the anion in the cubic unit cell; however, in AB_2X_4 compounds, only 24 are occupied by cations and 64 tetrahedral interstices that exist between the

anions, 8 are occupied by cations. The remaining 16 cations occupy half of the 32 octahedral interstices. The tetrahedral coordinate cations form a diamond cubic sublattice with a repeat unit equal to the lattice parameter. The periodicity associated with the sublattice of octahedral coordinate cations also is equal to a .

Atomic positions in spinel are dependent on the choice of setting for the origin in $\text{Fd}\bar{3}\text{m}$ space group. Two different equipoints with point symmetries $\bar{4}3\text{m}$ and $\bar{3}\text{m}$ are possible choices for the unit-cell origin. Moreover, the origin can be assigned to either a vacant site or an occupied lattice site. The equipoints for the various lattice sites are denoted using Wyckoff notation [9]. The conventional choices for the unit-cell origin in spinel are either $\bar{4}3\text{m}$ on an A-site cation or $\bar{3}\text{m}$ on an octahedral vacancy.

A-site tetrahedral in spinel is isolated from each other and share with neighboring octahedral B-site. But no edge sharing occurs between tetrahedral A-site and polyhedral A or B-site. Octahedral B-site share six of twelve X-X edges with nearest neighbor octahedral B-sites, that surround 16c vacant sites. The X-X edges that are shared by the B cations form chains in the lattice along the $\langle 110 \rangle$ directions. Because no intervening anions obstruct neighboring B-site cations, B-B distances are short, which facilitates electrical conductivity in some spinels, via electron hopping between B-sites [10].

B. X-Ray Diffraction Intensity

In order to determine the cation distribution, the X-ray intensities were calculated using the formula suggested by Burger [6],[8].

$$I_{hkl} = |F_{hkl}|^2 \cdot p \cdot L_p \quad (1)$$

where, I_{hkl} = Relative integrated intensity

F_{hkl} = Structure factor

p = Multiplicity factor

$$L_p = \text{Lorentz - polarization factor} = \frac{1 + \cos^2 2\theta}{\sin^2 \theta \cdot \cos \theta}$$

θ = Bragg's angle

Structure Factor (F_{hkl})

For calculating structure factor we have to consider atomic scattering factor [6]. Here the atomic scattering factor is used to describe the "efficiency" of scattering of a given atom in a given direction. It is defined as a ratio of amplitudes:

$$f = \frac{\text{amplitude of the wave scattered by an atom}}{\text{amplitude of the wave scattered by one electron}}$$

Atomic scattering factor depends on the Bragg angle θ and the wavelength of incident beam. At a fixed value of θ , f will be smaller the shorter the wavelength, since the path differences will be larger relative to the wavelength. The actual calculation of f involves $\sin\theta$ rather than θ , so that the net effect is that f decreases as quantity $\sin\theta/\lambda$ increases. The scattering factor f is sometimes called the form factor, because

it depends on the way in which the electrons are distributed around the nucleus. Now resultant wave scattered by all the atoms of the unit cell is called the structure factor, because it describes how the atom arrangement, given by uvw (cell parameters) for each atom, affects the scattered beam. The structure factor, designated by the symbol F, is obtained by simply adding together all the waves scattered by individual atoms. If a unit cell contains atoms 1,2,3...N, with fractional coordinates $u_1 \ v_1 \ w_1$, $u_2 \ v_2 \ w_2$, $u_3 \ v_3 \ w_3$... and atomic scattering factors f_1, f_2, f_3, \dots , then the structure factor for the hkl reflection is given by,

$$F = f_1 e^{2\pi i(hu_1 + kv_1 + lw_1)} + f_2 e^{2\pi i(hu_2 + kv_2 + lw_2)} + f_3 e^{2\pi i(hu_3 + kv_3 + lw_3)} + \dots$$

This equation may be written as,

$$F_{hkl} = \sum_{j=1}^N f_j e^{2\pi i(hu_j + kv_j + lw_j)} \quad (2)$$

Similarly, Structure Factor equations for all the Bragg planes of the spinel structure are as follow in Table I:

TABLE I
STRUCTURE FACTOR (F) EQUATIONS FOR DIFFERENT
BRAGG'S PLANE OF SPINEL STRUCTURE

Bragg's planes	Structure Factor
[111]	$4(-\sqrt{2}F_A + 2F_B)$
[220]	$-8F_A$
[311]	$4(-\sqrt{2}F_A - 2F_B)$
[222]	$(16F_B - 2F_O)$
[400]	$8(-F_A + 2F_B + 4F_O)$
[422]	$8F_A$
[333]	$4(\sqrt{2}F_A + 2F_B)$
[511]	$4(\sqrt{2}F_A - 2F_B)$
[440]	$8(F_A + 2F_B + 4F_O)$
[531]	$4(\sqrt{2}F_A - 2F_B)$
[111]	$4(-\sqrt{2}F_A + 2F_B)$
[220]	$-8F_A$
[311]	$4(-\sqrt{2}F_A - 2F_B)$
[222]	$(16F_B - 2F_O)$
[400]	$8(-F_A + 2F_B + 4F_O)$

where f_A , f_B and f_O are structure factors for A-site cations, B-site cations and anions respectively.

Multiplicity Factor (p)

The relative proportion of planes contributing to the same reflection enters the intensity equation as the quantity p may be defined as the number of different planes in a form having the same spacing [6]. The value of the multiplicity factors (p) as function of (hkl) and crystal system are given below:

Lorentz Polarization Factor (L_p)

In intensity calculations, the Lorentz factor is given as below;

$$\text{Lorentz factor} = \left(\frac{1}{\sin 2\theta} \right) (\cos \theta) \left(\frac{1}{\sin 2\theta} \right)$$

This in turn is combined with the polarization factor $\frac{1}{2}(1 + \cos^2 2\theta)$ to give the combined Lorentz polarization factor which, with a constant factor of 1/8 omitted, Lorentz-polarization factor [6]:

$$\text{Lorentz factor}(L_p) = \frac{1}{4\sin^2 \theta \cos \theta} = \frac{1 + \cos^2 2\theta}{\sin^2 \theta \cos \theta}$$

C. Input File Format for the XRD Intensity Analysis Computer Program

The input file is in .txt form having following formation;

```
Mg0.6Zn0.4Fe2-xAlxO4
0.3
5
Mg Zn Al Fe O-2
0.00 0.60
0.40 0.00
0.00 0.30
0.60 1.10
0.00 0.00
1.93998
220 40.410 37.8173
311 100.00 44.7128
400 15.720 54.6765
422 12.270 68.5392
511 21.630 73.3727
440 44.660 81.1739
999 6
220 440
400 422
220 400
```

The X-ray diffraction intensity of six Bragg's reflections (220), (311), (400), (422), (511) and (440) was calculated by running the computer program of X-ray diffraction intensity calculation (INTENSITY.exe) for spinel structure. To deduce final cation distribution, simply one has to insert input file name (input file format is shown as above) and to generate output file of result. The result for composition $x = 0.3$ for $\text{Mg}_{0.6}\text{Zn}_{0.4}\text{Fe}_{2-x}\text{Al}_x\text{O}_4$ spinel ferrite system shown in Table III.

In fact, the program developed for the XRD intensity calculation can calculate XRD intensity of all the allowed Bragg's planes for the fcc spinel structure but only six Bragg's planes which are most sensitive to the cation distribution have been considered.

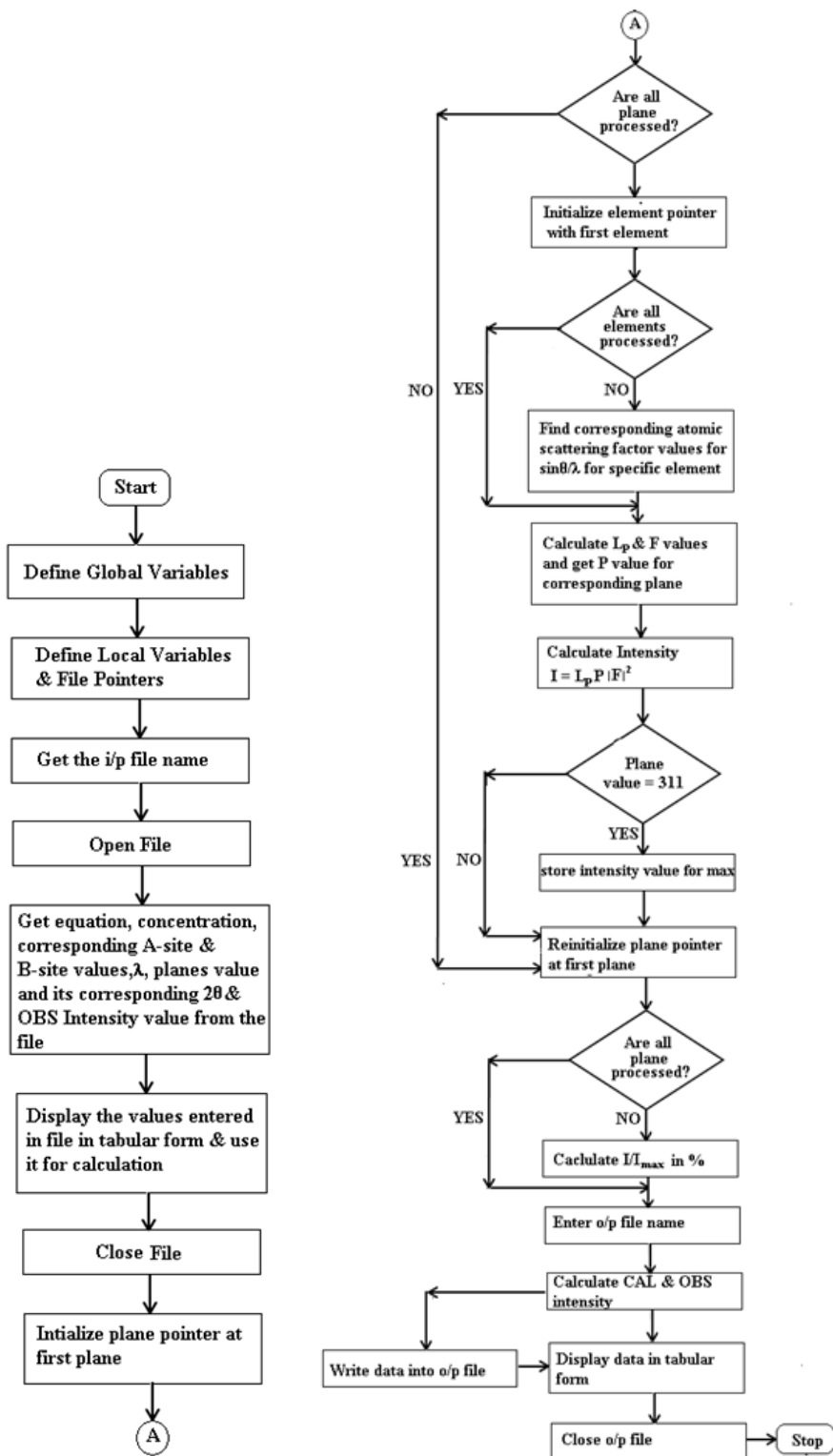


Fig. 2 Flowchart for XRD intensity analysis computer program

III. EXPERIMENTAL DETAILS

The samples of spinel ferrite $\text{Mg}_{0.6}\text{Zn}_{0.4}\text{Al}_x\text{Fe}_{2-x}\text{O}_4$ ($x=0.1$ to 0.6 , step = 0.1) were synthesized by standard ceramic technique [11] by prolonged heating of the oxide ingredients followed by slow programmed cooling to room temperature. The ferrites were characterized using FeK_α radiation by X-ray diffraction (Model: Philips, PW 1820) at 300K . X-ray diffraction patterns of all the Spinel Ferrite samples clearly indicated the presence of the face centered cubic (fcc) phase (Fig. 3). The saturation magnetization (σ_s) for each sample of $\text{Mg}_{1-x}\text{Zn}_x\text{Fe}_2\text{O}_4$ and $\text{Mg}_{0.6}\text{Zn}_{0.4}\text{Fe}_{2-x}\text{Al}_x\text{O}_4$ ($x=0.1$ to 0.6) measured at 77K in the peak field of 5 kOe using high field hysteresis loop tracer [12]. The Neel temperature (T_N in K) determined for all the samples through low field AC Susceptibility measurements using the double coil setup [13]. The compositional and temperature dependence of d.c. electrical resistivity measurements studied for the present spinel ferrite system.

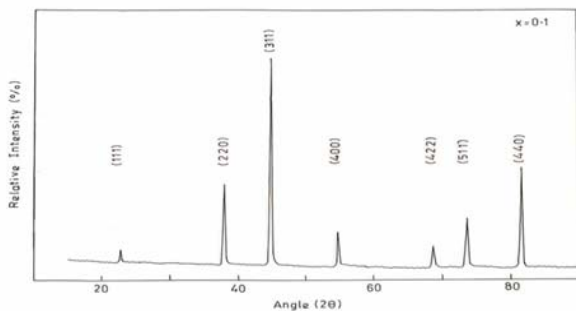


Fig. 3 Typical X-ray diffraction patterns for $\text{Zn}_{0.4}\text{Mg}_{0.6}\text{Al}_{0.1}\text{Fe}_{1.9}\text{O}_4$

IV. RESULT AND DISCUSSION

According to Ohnishi and Teranishi [14] the intensity ration of planes $I(220)/I(400)$ and $I(400)/I(422)$ are considered to be sensitive to the cation distribution parameters (x). The ionic configuration based on site preference energy values proposed by Miller [15] for individual cations in $\text{Zn}_{0.4}\text{Mg}_{0.6}\text{Al}_x\text{Fe}_{2-x}\text{O}_4$ suggests that Zn^{2+} occupies A-site, Al^{3+} occupies only B-sites where as Mg^{2+} and Fe^{3+} ions occupy A-and B-sites. The Fe^{3+} ion is having good contrast in the atomic scattering factors with other cations present in the system. This makes the determination of cation distribution quite reliable. Moreover, any alternation in the distribution of cations causes significant change in the theoretical values of X-ray diffraction intensity ration. Therefore, in the process of arriving at final cation distribution, the site occupancy of all the cations was varied for many combinations and deduced final distribution for the present system. In the spinel ferrite system $\text{Mg}_{1-x}\text{Zn}_x\text{Fe}_2\text{O}_4$ [16], the saturation magnetization (σ_s) increases up to $x=0.4$ with increase in Zn-concentration then decreases on further Zn-addition. While it decreases monotonously with increase in Al-content for $\text{Mg}_{0.6}\text{Zn}_{0.4}\text{Fe}_{2-x}\text{Al}_x\text{O}_4$ (Table IV). The Neel temperature values for all the specimens (Fig. 4) lie in temperature range $800\text{ K} - 350\text{ K}$ (Table V), which gives the

value of T/T_N ration at 77K for each specimen ~ 0.2 . The Neel temperature (T_N) estimated through the following equation.

$$T_N(x) = \left[\frac{p(x)}{p(x=0)} \right] T_N(x=0) \quad (3)$$

It is found that the rate of decrease of T_N for Zn-addition in $\text{Mg}_{1-x}\text{Zn}_x\text{Fe}_2\text{O}_4$ [16] is steeper compared with this case of Al-substitution in $\text{Mg}_{0.6}\text{Zn}_{0.4}\text{Al}_x\text{Fe}_{2-x}\text{O}_4$ system indicating less dilution of A-B interactions due to Al-substitution. The agreement of theoretically calculated T_N (Table V) with experimentally determined values clearly supports the cation distribution deduced through the XRD intensity calculations. The value of T/T_N ration at $T=300\text{ K}$ is about 0.6 which is very poor for magnetic measurements as suggested by the Brillouin function [17]. Therefore, the magnetization data recorded at 77 K for the present system are valid for the calculation of magneton number (n_B) i.e. saturation magnetization per formula unit in Bohr Magneton at absolute zero temperature. The n_B was calculated from bulk magnetization values to extract microscopic information using formula:

$$n_B^{obs} (\text{Bohr magneton}) = \left\{ \frac{\text{molecular weight}}{5585} \right\} \sigma_s \left(\frac{\text{emu}}{\text{g}} \right) \quad (4)$$

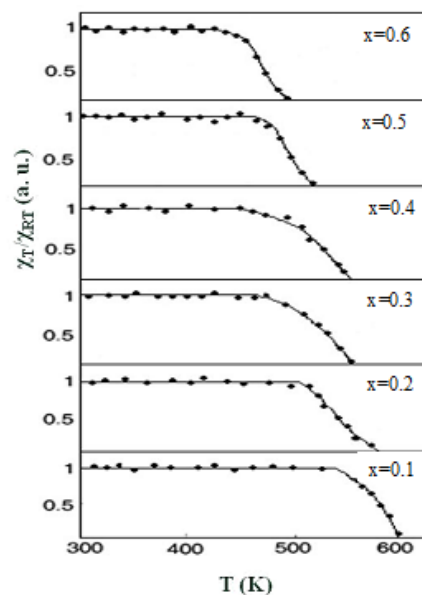


Fig. 4 Thermal variation of AC susceptibility for the system: $\text{Zn}_{0.4}\text{Mg}_{0.6}\text{Al}_x\text{Fe}_{2-x}\text{O}_4$

TABLE III
X-RAY DIFFRACTION INTENSITY CALCULATION COMPUTER PROGRAM OUTPUT FILE

2θ	PLANE	L	P	F	I	CALC%	OBS%
37.8173	220	16.33	12	30158.58	5910809.50	40.96	40.41
44.7128	311	11.24	24	53495.94	14428071.0	100.0	100.0
54.6765	400	7.12	6	47884.34	2044341.62	14.16	15.72
68.5392	422	4.32	24	18796.42	1950486.12	13.51	12.27
73.3727	511	3.78	24	35364.82	3205686.00	22.21	21.63
81.1739	440	3.18	12	173658.6	6631561.50	45.96	44.66

RATIO CALCULATION		
PLANE	CAL	OBS
220/440	0.8913	0.9048
400/422	1.0481	1.2812
220/400	2.8913	2.5706

The values of magneton number calculated on the basis of the cation distribution determined through the XRD intensity calculation and the Neel's two sublattice model, i.e. Neel's moment, $n_B^N = M_B - M_A$, (where M_B and M_A are sublattice magnetizations) for both the systems are listed in Table.1. The discrepancy between the Neel's moment and observed moment increase of $Mg_{1-x}Zn_xFe_2O_4$ after $x = 0.4$ suggests the non-collinear or canted spin structure. The initial composition $Mg_{0.6}Zn_{0.4}Fe_2O_4$ of other system $Mg_{0.6}Zn_{0.4}Fe_{2-x}Al_xO_4$ showed the onset of canted spin structure (Table IV). Using the localized canting of spins (LCS) model of Patton and Liu [5] the average canting angle θ_{L-AV} (Table IV) can be calculated for both the systems: $Mg_{1-x}Zn_xFe_2O_4$ and $Mg_{0.6}Zn_{0.4}Fe_{2-x}Al_xO_4$. From the cation distribution deduced through X-ray diffraction intensity calculation, the LCS equations are obtained for the systems $Mg_{1-x}Zn_xFe_2O_4$ and $Mg_{0.6}Zn_{0.4}Fe_{2-x}Al_xO_4$ can be derived as,

$Mg_{1-x}Zn_xFe_2O_4$:

$$\cos \theta_{L-AV} = \frac{2(1-x)}{1+x} \left| \frac{JAB_i}{JBB_i} \right| \quad (5)$$

$Mg_{0.6}Zn_{0.4}Fe_{2-x}Al_xO_4$:

$$\cos \theta_{L-AV} = \frac{1.2}{1.4-x} \left| \frac{JAB_i}{JBB_i} \right| \quad (6)$$

The electrical resistivity as function of temperature for the three composition of system $Zn_{0.4}Mg_{0.6}Al_xFe_{2-x}O_4$ in the form of Arrhenius plots of $\log \rho$ versus $10^3/T$ shown in Fig. 5. The value of ρ increases with increase in Al-concentration (x) (Fig. 6). The most probable conduction mechanism in these materials is through electron hopping between Fe^{2+} and Fe^{3+} ions. This process is expected to occur between two adjacent octahedral sites in spinel lattice. Thus, the increase in the electrical resistivity with Al-substitution is due to the replacement of Fe^{3+} by Al^{3+} which dilutes the conduction through the octahedral sites.

Temperature dependence of electrical resistivity is given by following Arrhenius equation. The slope of these plots change at Neel temperature.

TABLE IV
SATURATION MAGNETIZATION (σ_s), MAGNETON NUMBER (N_B) AND CANTING ANGLE (θ_{L-AV})

$Mg_{1-x}Zn_xFe_2O_4$					
Content (x)	σ_s (emu/g) at 77 K	n_B^N (μ_B)	n_B^{obs} (μ_B)	θ_{L-AV} CALC	n_B^L (μ_B)
0.0	30	1.0	1.07	0	1.00
0.1	41	1.0	1.51	0	1.00
0.2	60	2.0	2.24	0	2.00
0.3	78	3.0	3.05	0	3.00
0.4	82	4.0	3.18	25° 50'	3.30
0.5	75	5.0	2.96	45° 34'	2.75
0.6	54	6.0	2.17	58° 20'	2.20
0.7	40	7.0	1.63	68° 15'	1.65
0.8	28	8.0	1.17	76° 30'	1.10
0.9	11	9.0	0.47	84° 39'	0.55

$Mg_{0.6}Zn_{0.4}Fe_{2-x}Al_xO_4$					
0.0	82	4.0	3.18	25° 50'	3.30
0.1	84	3.5	3.23	14° 15'	3.30
0.2	80	3.0	3.00	Collinear	-
0.3	67	2.5	2.49	Collinear	-
0.4	54	2.0	1.98	Collinear	-
0.5	41	1.5	1.50	Collinear	-
0.6	27	1.0	0.98	Collinear	-

$$\rho = \rho_0 \exp \left[\frac{\Delta E}{kT} \right] \quad (7)$$

where, k is Boltzmann's constant and ΔE is the activation energy.

The activation energy increases on changing from the ferrimagnetic (ΔE_f) to the paramagnetic (ΔE_p) region (Table VI). The values of T_N are in good agreement with values determined through AC susceptibility measurement and the theoretically estimated.

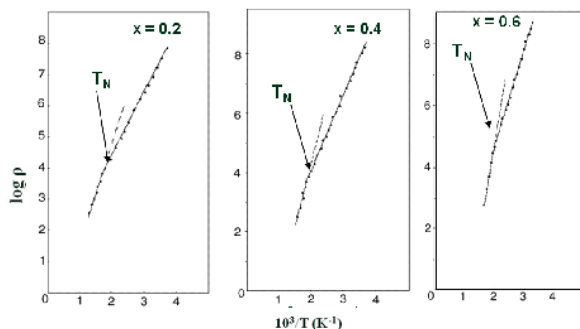


Fig. 5 Electrical resistivity versus temperature for the system:
 $\text{Zn}_{0.4}\text{Mg}_{0.6}\text{Al}_x\text{Fe}_{1-x}\text{O}_4$

TABLE V
NEEL TEMPERATURE: MEASURED AND THEORETICALLY
CALCULATED FOR THE SYSTEM: $\text{Mg}_{0.6}\text{Zn}_{0.4}\text{Fe}_{2-x}\text{Al}_x\text{O}_4$

Content (x)	T_N (K)		Calculated T_N (K)
	Measured Susceptibility	Resistivity	
0.0	610	590	610
0.1	595	-	596
0.2	580	588	581
0.3	560	-	564
0.4	540	541	544
0.5	520	-	523
0.6	490	500	498

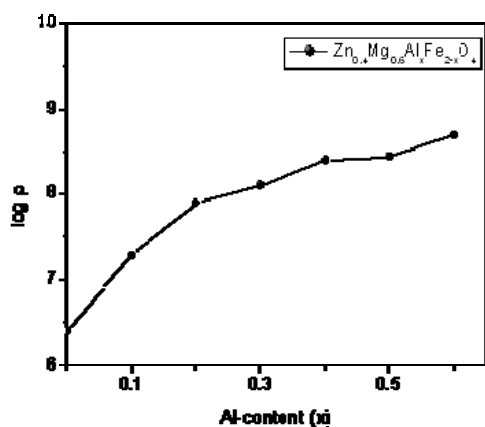


Fig. 6 Electrical resistivity versus Al-content for the system:
 $\text{Zn}_{0.4}\text{Mg}_{0.6}\text{Al}_x\text{Fe}_{1-x}\text{O}_4$

TABLE VI
THE ACTIVATION ENERGY FOR FERRIMAGNETIC (ΔE_f) AND
PARAMAGNETIC (ΔE_p) REGIONS FOR THE SYSTEM:
 $\text{Mg}_{0.6}\text{Zn}_{0.4}\text{Fe}_{2-x}\text{Al}_x\text{O}_4$

Content (x)	Activation Energy (eV)	
	Ferrimagnetic (ΔE_f)	Paramagnetic (ΔE_p)
0.2	0.61	0.41
0.4	0.93	0.49
0.6	1.13	0.61

V. CONCLUSION

The developed XRD intensity calculation program worked well for the synthesized system $\text{Zn}_{0.4}\text{Mg}_{0.6}\text{Al}_x\text{Fe}_{2-x}\text{O}_4$. The program shall prove to be very useful to the students and for quick check of cation distribution to researchers. The localized canting of spins model fits the magnetization data well and the magnetic ordering found for the system supports the cation distribution determined through the XRD intensity calculations. The agreement of theoretical Neel Temperature (T_N) and its experimentally observed value supports the cation distribution and therefore validity of the computer program.

REFERENCES

- [1] L. Neel, "Propriétés magnétiques des ferrites; Férrimagnétisme et antiferromagnétisme," *Annales de Physique*, Paris, vol. 3, pp. 137-198, 1948.
- [2] Y. Yafet and C. Kittel, "Antiferromagnetic arrangements in ferrites," *Physical Review*, vol. 87, no. 2, pp. 290-294, March 1952.
- [3] A. Rosencwaig, "Localized canting model for substituted ferrimagnets. I. Singly substituted YIG systems," *Can. J. Physics*, vol. 48, pp. 2857-2867, Dec. 1970.
- [4] A. Rosencwaig, "Localized canting model for substituted ferrimagnets. II. Doubly substituted YIG systems," *Can. J. Physics*, vol. 48, pp. 2868-2876, Dec. 1970.
- [5] C. E. Patton and Yi-hua Liu, "Localized canting models for substituted magnetic oxides," *J. Phys. C: Solid State Phys.*, vol. 16, pp. 5995-6010, Nov. 1983.
- [6] B.D. Cullity, *Elements of X-ray diffraction II Edition*, Addison-Wesley Pub. Co., 1978, ch. 4.
- [7] S.K. Chatterjee, "X-ray diffraction- its theory and applications," PHI, 1999, ch. 3.
- [8] W. H. Bragg, "The structure of the spinel group of crystals," *Phil. Mag.*, vol. 30, pp. 305-315, Aug. 1915.
- [9] S. Krupicka and P. Novak, "Ferromagnetic materials," Vol. 3 North-Holland Publishing Co. New York, 1982, ch. 4.
- [10] K. E. Sickafus, J. M. Wills and N. W. Grimes, "Structure of Spinel," *J. Am. Ceram. Soc.*, vol. 82, no. 12, pp. 3279-3292, Dec. 1999.
- [11] K.J. Standly, "Oxide Magnetic Materials," Clarendon press, Oxford, 1962, ch. 2.
- [12] C. Radhakrishnamurty, S.D. Likhite and N.P. Sastry, "Low temperature magnetic hysteresis of fine particle aggregates occurring in some natural samples," *Philos. Mag.*, vol. 23, pp. 503-507, Feb. 1971.
- [13] S.D. Likhite and C. Radhakrishnamurty, "Initial Susceptibility and Constricted Rayleigh Loops of some Basalts," *Curr. Sci.*, vol. 35, pp. 534-536, Nov. 1966.
- [14] H. Ohnishi, T. Teranishi, "Crystal Distortion in Copper Ferrite-Chromite Series," *J. Phys. Soc. Jpn.*, vol. 16, pp. 35-43, Jan. 1961.
- [15] A. Miller, "Distribution of Cations in Spinel," *J. Appl. Phys.*, vol. 30, pp. S24-S25, Apr. 1959.
- [16] H. H. Joshi and R. G. Kulkarni, "Susceptibility, magnetization and Mossbauer studies of the Mg-Zn ferrite system," *J. Materials Sci.* vol. 21, no. 6, pp. 2138-2142, June 1986.
- [17] B.D. Cullity, "Introduction to magnetic materials," Addison Wesley, 1972, ch. 4.

Mr. Ashish R. Tanna has received M.Sc. (Physics) with specialization in Electronics & Communication in 2003 and M. Phil in 2004 in Material Science. As a part of his M.Phil work, he has developed variety of computer software for materials scientists working in the field of magnetism. He is pursuing his Ph.D. on the study of ferrite-ferroelectric (multiferroic) composites with emphasis on the influence of high energy mechanical milling on their transport properties. He has developed expertise in computer simulation and ceramic processing of materials. He is working as Assistant Professor at School of Engineering, R.K University, Rajkot, India, since 2005. He has presented and published quite a few research papers at international conferences and journals. He has authored two books on materials science & engineering.

Dr. Hiren H. Joshi has received M.Sc. (Physics) with specialization in Electronic Communication in 1982 and Ph.D. in Materials science (fine particle magnetism) in 1987 from Saurashtra University, Rajkot, India. He has expertise in synthesis of nano-structured ferrites, ceramic processing, magnetic ordering modeling, X-ray crystallography, neutron diffraction and Mossbauer spectroscopy. He has more than 100 research papers published in international journals. He has guided 11 M.Phil and 7 Ph.D. students. At present 4 Ph.D. students working under his guidance. He has 26 years of post graduate teaching and research experience. At present he is Professor and Head of Department of Physics, Saurashtra University, Rajkot, India.